Structural Damage Detection and Calibration Using Wavelet-Kurtosis Technique

V. Pakrashi, B. Basu and A. O' Connor

Department of Civil, Structural and Environmental Engineering, Trinity College Dublin

Abstract

Some key factors in the field of damage detection of structures are the efficient and consistent detection of the presence, location and the extent of damage. A detailed numerical study has been performed in this paper addressing these issues for a beam element with an open crack. The first natural modeshape of the beam with an open crack has been simulated using smeared, lumped and continuous crack models involving various degrees of complexity. The static deflected shape of the same beam has also been simulated under vertical static loading. Gaussian white noise of different intensities has been synthetically introduced to both the simulated damaged modeshape and the static deflected shape. Wavelet analysis has been performed on the simulated modeshape and the static deflected shape for locating the damage. A new wavelet-kurtosis based calibration of the extent of damage have been performed for different crack depth ratios and crack positions including the effects of varying signal to noise ratio. An experimental validation of this method has been carried out on a damaged aluminium beam with open cracks of different extent. The damaged shape has been estimated by using a novel video camera based pattern recognition technique. The study in this paper shows that wavelet analysis in conjunction with a kurtosis based damage calibration can be useful in the

identification of damage to structures and is applicable under the presence of measurement noise.

Keywords
Open Crack, Wavelets, Signal to Noise Ratio, Kurtosis, Windowing, Masking

1. Introduction

Identification of change in natural frequencies and modeshapes of a freely vibrating damaged beam with respect to its undamaged state has traditionally been a popular method for damage identification. These changes are often quite small and the method performs poorly when measurements are contaminated by noise. Analysis of damaged modeshapes by wavelet transform provides a better and more robust methodology for the identification of damage. A sharp change in the wavelet coefficients at different scales near the damage location indicates the presence and the location of the damage while the magnitude of the local extrema of the wavelet coefficients at the location of damage can be related to the extent of the damage. The principles behind such wavelet based damage detection are associated with the detection of singularities in a function or in any of its derivatives. Hence, information about the beam in its undamaged state is not required.

The aspect of singularity detection through wavelets has been discussed in details by Mallat [1]. Gentile and Messina [2] have discussed the criteria for a proper selection of wavelet basis functions to efficiently identify the damage in a beam with an open crack in the presence of measurement noise and have demonstrated the performances of Gaussian and Symlet wavelets in the detection process. Loutridis et al [3], Chang and Chen [4] and Okafor and Dutta [5] have considered the problem of the identification of open cracks in a beam as well, but with a single type of wavelet basis function for analysing the damaged modeshapes. Melhem and Kim [6] have analysed the response of concrete structures and have shown the effectiveness of using wavelet transform over traditional Fourier transform in identification of damage. Kim and Melhem [7] have demonstrated the versatile use of the wavelet based method through application on

damages related to mechanical gears and rollers. Spatial response data from beam structures have been successfully analysed by wavelets to detect damage by Wang and Deng [8]. Hou et al. [9] have employed a wavelet analysis based scheme to detect accumulated damage occurrence in a structure modelled by a multiple breakable spring and validated it with the application of a recorded ground accelerogram of the 1971 San Fernando earthquake. Basu [10] demonstrated that a wavelet based structural health monitoring technique for a stiffness degrading structure is very effective and can be used even without any a-priori knowledge of the original structural system. In this regard, a modified form of Littlewood Paley basis function was employed for the analysis and examples were presented for a bi-linear structure with breakable springs and a hysteretic system with continuous variation of stiffness with nonlinearity involving displacement and velocity response. Advantages of wavelet analysis over the usual eigenvalue analysis for a simply supported beam with a non-propagating open crack have been shown by Liew and Wang [11]. Moyo and Brownjohn [12] have used wavelet analysis on a bridge structure to improve structural health monitoring since this method successfully detects abrupt changes and gradual change at the beginning and at the end of an event.

It is observed that although the detection of an open crack in a beam has been comparatively well dealt with, few studies have been performed to calibrate the extent of damage. Hadjileontiadis et al. [13, 14] tried to detect and quantify the damage by fractal dimension analysis and by a kurtosis crack detection scheme for a cantilever with an open crack. The schemes were comprised of analysing each part of the modeshape signal with sliding overlapping windows of a certain width along the spatial data. However, to have a successful identification of damage the number of the windows, the width of each

window and the overlapping of windows were empirically chosen. This requires prior knowledge about the crack and the calibration is only possible after a proper empirical choice of windows. The resistance to the effect of noise was not calibrated either. Hence, there is a necessity of quantifying the extent of damage in a robust and efficient way apart from detecting the damage location correctly.

This paper considers a simply supported Euler Bernoulli beam with an open crack. Different crack models involving various levels of complexity have been considered to illustrate the potential use of a wavelet based method. This proposed method is independent of any chosen damage model as long as there is a sharp local change in the resulting damaged shape or in any of its derivatives. The popular lumped crack model that considers a rotational spring at the location of damage has been considered as per Narkis [15], Masoud et al [16], Dado [17], Hadjileontiadis et al [13, 14] and Loutridis et al [3]. A much more complex and sophisticated continuous cracked beam modelling based on Hu – Washizu – Barr mixed variational principle has been performed following Carneiro [18, 19], which is a modification of the model considered by Shen and Pierre [20] and Christides and Barr [21]. In addition to these two damage models, a third and more simplistic smeared crack model has been considered by treating the open crack as a reduced moment of inertia over the damaged width.

A new wavelet-kurtosis based approach has been proposed to identify and calibrate the damage. Wavelet analysis has been performed on the simulated modeshape and static deflected shape data considering the effects of windowing and presence of noise, followed by kurtosis analysis. Cracks of different sizes and locations have been used in the presented examples. The proposed method has been validated experimentally

by performing wavelet analysis on the damaged shape of a simply supported freely vibrating aluminium beam.

2. Damage Modelling

2.1 Lumped Crack Model

A simply supported Euler Bernoulli beam with an open crack is modelled as two uncracked beams connected through a rotational spring at the location of crack. The length of the beam is L with the damage located at a distance of '*a*' from the left hand support of the beam. The crack depth is taken as *c* and the overall depth of the beam is *h*. The free vibration equation for both the beams on either side of the crack can be written as

$$EI\frac{\partial^4 y}{\partial x^4}+\rho A\frac{\partial^2 y}{\partial t^2}=0 \qquad (1)$$

where E, I, A and ρ are the Young's modulus, the moment of inertia, the cross sectional area and the density of the material of the beam on either side of the crack. The displacement of the beam from its static equilibrium position is y(x,t), at a distance of x from the left hand support along the length of the beam at time t. It is assumed that the effects of the crack are applicable in the immediate neighbourhood of the crack location and are represented by a rotational spring. By separation of variables in Equation 1 and solving the characteristic equation, a general solution of the modeshapes is found as

$$\Phi_L = C_{1L}Sin(\lambda x)+C_{2L}Cos(\lambda x)+C_{3L}Sinh(\lambda x)+C_{4L}Cosh(\lambda x) \qquad 0 \le x < a \quad (2.1)$$

and

$$\Phi_R = C_{1R}Sin(\lambda x)+C_{2R}Cos(\lambda x)+C_{3R}Sinh(\lambda x)+C_{4R}Cosh(\lambda x) \qquad a \le x \le L \quad (2.2)$$

for the sub-beams on the left and the right side of the rotational spring respectively. The terms $C_{(.)}$ are integration constants arising from the solution of the separated fourth order differential equation in space. The term λ is expressed as

$$\lambda = (\frac{\rho A \omega^2}{EI})^{1/4} \tag{3}$$

where the natural frequency of the cracked beam is ω. Both the displacement and the moment at the two supports of the beam are zero. Hence

$$\Phi_L(0) = 0 \ , \Phi_L''(0) = 0 , \ \ \Phi_R(L) = 0 \ \text{ and } \ \Phi_R''(L) = 0 \tag{4.1}$$

The continuity in displacement, moment and shear are assumed at the location of crack. These conditions can be expressed as

$$\Phi_L(a) = \Phi_R(a) , \ \Phi_L''(a) = \Phi_R''(a) \text{ and } \Phi_L'''(a) = \Phi_R'''(a) \tag{4.2}$$

A slope discontinuity is introduced at the crack location. The slope condition is modelled as

$$\Phi_R'(a) - \Phi_L'(a) = \theta L \Phi_R''(a) \tag{4.3}$$

In equation 4.3, the term θ is the non-dimensional crack section flexibility dependent on the crack depth ratio, δ(=a/h). As per Narkis [15], the term θ is considered to be a polynomial of δ as

$$\theta = 6\pi\delta^2(h/L)(0.5033 - 0.9022\delta + 3.412\delta^2 - 3.181\delta^3 + 5.793\delta^4) \tag{5}$$

The boundary conditions are substituted in the general modeshape equation and a system of eight linear equations is formed. The natural frequency of the cracked beam may be found by setting the determinant of the matrix derived from the system of equations to zero, expanding it and solving for the roots of λ numerically. In this paper, the roots were

found using Brent's method in MATLAB. The coefficient C_{1L} is normalized to unity, being consistent with the fact that for an undamaged beam the maximum of the first modeshape is equal to unity. The other coefficients are then found with respect to C_{1L}.

2.2 Continuous Crack Model

The continuous crack model is derived by Carneiro [18, 19] from the stationarity of Hu-Washizu-Barr functional [21] and is a refined version of the proposed model by Shen and Pierre [20] ensuring the self-adjointness of the differential operator for a symmetric matrix representation after the discretization of the free vibration equation. The model is described briefly in this section for the sake of completeness. The functional is represented as

$$J = \int_{t_1}^{t_2} \{ \int_V [\rho p_i \dot{u}_i - \hat{T}(p_i) - W(\varepsilon_{ij}) + (\varepsilon_{ij} - \frac{1}{2}(u_{i,j} + u_{j,i}))\sigma_{ij}\} dV + \int_{S_1} \bar{g}_i u_i dS_1 + \int_{S_2} (u_i - \bar{u}_i) g_i dS_2] \} dt \quad (6)$$

In equation 6, the terms $u_{(.)}$, $p_{(.)}$ $\varepsilon_{(.)}(.)$, $\sigma_{(.)}(.)$, $g_{(.)}$, $W(.)$ and $\hat{T}(.)$ represent the displacements, velocities, strains, stresses, surface tractions, strain energy density and kinetic energy density of the beam respectively. The prescribed values are denoted by overbars and are defined over complementary surfaces S_1 and S_2 for traction and displacements respectively for the beam of volume V. The indexes i and j represent directions with respect to the origin and denote the Cartesian coordinates represented by the subscripts 1,2 and 3 respectively. The origin is at the extreme left hand corner and equidistant from the top and bottom surface of the beam. The coordinate axes x and y and z denote directions along the length, the width and the depth of the beam respectively. The stationarity of the functional is considered between two arbitrarily chosen time

instants t_1 and t_2. The first variation of the functional is set to zero with respect to independent variations of u_i, p_i, ε_{ij} and σ_{ij}. For a rectangular cross section, the stress-strain and the displacement functions are assumed to be locally disturbed in the vicinity of the crack. The effect of the crack is considered maximum at the crack tip and decays exponentially away from it. The stress/strain disturbance function is assumed to be

$$f_1(x,z) = [z - m_1(z + c/2)H(h/2 - c - z)]e^{-\alpha_1 \frac{|x-a|}{h/2}} \tag{7.1}$$

where m_1 is a factor computed considering the continuity of bending moment in the cracked section and α_1 denotes the stress decay parameter. The term H(.) is the Heaviside step function. The displacement disturbance function is similar and considered as

$$f_2(x,z) = [z - (z + c/2)H(h/2 - a - z)]e^{-\beta_1 \frac{|x-a|}{h/2}} \tag{7.2}$$

The decay factor β_1 is much steeper than that of the stress/strain disturbance function. The equation of motion for the free vibration of the beam considering these kinematic assumptions is given as

$$E[p_2(x)\xi(x,t)'']'' + E[p_1(x)\xi(x,t)']' + \rho A\ddot{\xi}(x,t) = 0 \tag{8}$$

where $\xi(x,t)$ is the vertical displacement of the beam and the primes and overdots represent differentiation with respect to the space and time respectively. The terms $p_1(x)$ and $p_2(x)$ are given in Appendix1. Separation of variables is performed and a Galerkin approximate solution is sought to the eigenvalue problem by expanding the transverse deflection as a combination of N number of mutually orthogonal uncracked modes of vibration. Thus,

$$\xi(x,t) = W(x)\eta(t) \tag{9.1}$$

$$W(x) = \sum_{i=1}^{N} C_i \mathrm{Sin}\left(\frac{i\pi x}{L}\right) \tag{9.2}$$

In equation 9.1, W(x) and $\eta(t)$ denote the spatial and the temporal part of the lateral displacement respectively. Substituting equation 9.2 in equation 8 and considering the orthogonality of the modeshapes, the mass and the stiffness matrix for the system can be written as

$$[M_{ij}] = \int_0^L \rho A \mathrm{Sin}\left(\frac{i\pi x}{L}\right)\mathrm{Sin}\left(\frac{j\pi x}{L}\right)dx \tag{10.1}$$

$$[K_{ij}] = \int_0^L (\Gamma \mathrm{Sin}\left(\frac{i\pi x}{L}\right))\mathrm{Sin}\left(\frac{j\pi x}{L}\right)dx \tag{10.2}$$

where the operator Γ is

$$\Gamma = E\frac{\partial^2}{\partial x^2}\left([p_2(x)\frac{\partial^2}{\partial x^2}]\right) + E\frac{\partial}{\partial x}\left([p_1(x)\frac{\partial}{\partial x}]\right) \tag{11.1}$$

and

$$\Gamma(W(x)) = \hat{\lambda}(\rho A)W(x) \tag{11.2}$$

where $\hat{\lambda}$ is the eigenvalue of the problem and is the square of the natural frequency.

2.3 Smeared Crack Model

The smeared crack model is relatively simple and considers an open crack reducing the moment of inertia over an affected width. The governing free vibration equation is exactly the same as in equation 1. The damaged beam is analysed as an assembly of three sub-beams, the damaged sub-beam being positioned in between the two undamaged ones.

Continuity in deflection, slope, moment and shear are assumed on both left and right ends of the damaged zone. The boundary conditions considering a simply supported beam can thus be expressed as

$$\Phi_L(0) = 0, \Phi_L''(0) = 0 \ , \ \Phi_R(L) = 0, \Phi_R''(L) = 0 \tag{12.1}$$

$$\Phi_L(x_1) = \Phi_D(x_1), \Phi_L'(x_1) = \Phi_D'(x_1), \Phi_L''(x_1) = \Phi_D''(x_1), \Phi_L'''(x_1) = \Phi_D'''(x_1) \tag{12.2}$$

$$\Phi_R(x_2) = \Phi_D(x_2), \Phi_R'(x_2) = \Phi_D'(x_2), \Phi_R''(x_2) = \Phi_D''(x_2), \Phi_R'''(x_2) = \Phi_D'''(x_2) \tag{12.3}$$

where x_1 and x_2 denote the coordinates of the near and the far ends of the damaged zone respectively with reference to the origin situated on the extreme left hand side of the beam. The system of equations corresponding to the modeshapes and the continuity conditions give rise to a characteristic matrix, the determinant of which can be set to zero and solved for the natural frequencies of the damaged beam. The coefficients are found in the same way as of the lumped crack model. The width of the crack is computed according to the formula by Bovsunovsky and Matveev [22] as

$$\Delta x = x_2 - x_1 = \frac{0.3675h(1-\delta)}{1-(1-\delta)^3}[(1-\delta)^6 - 3(1-\delta)^2 + 2] \tag{13}$$

A discontinuity in the modeshape or in any of its derivatives is present in a damaged beam for any model of crack. Since a wavelet transform can successfully detect singularities in a signal or its derivatives, a wavelet based damage identification scheme is considered to be model independent and robust. Simulations of the first modeshape are used since it is convenient to measure the fundamental modeshape for real structures.

3. Static Deflection

Rucka and Wilde [23] have experimentally shown that the static deflection profile of a damaged beam can be analysed using wavelet transform to identify the location of the damage. Hence, instead of the modeshapes the static deflection profile of the beam with an open crack using the smeared and the lumped crack models have also been studied in this paper for the detection of damage.

Let the curvature of the beam be a piecewise integrable function $\gamma(x)$. The static deflection y(x) can thus be found as

$$y_L(x) = \int (\int \gamma(x)dx)dx + C_1 x + C_2 \tag{14.1}$$

$$y_R(x) = \int (\int \gamma(x)dx)dx + C_3 x + C_4 \tag{14.2}$$

where C_i are the constants of integration. A system of algebraic equations can be arrived at by satisfying the boundary conditions and the constants C_i may be solved from the following relationship

$$\begin{bmatrix} 0 & 1 & 0 & 0 \\ 0 & 0 & L & 1 \\ a & 1 & -a & -1 \\ -1 & 0 & 1 & 0 \end{bmatrix} \begin{Bmatrix} C_1 \\ C_2 \\ C_3 \\ C_4 \end{Bmatrix} = \begin{Bmatrix} 0 \\ -(\int (\int \gamma(x)dx)dx)\,|_L \\ 0 \\ \theta L(\int (\int \gamma(x)dx)dx)\,|_a \end{Bmatrix} \tag{15}$$

where $|_{(.)}$ denotes the evaluation of the integral at the location indicated within the parentheses. The solution of the static deflected shape introduces a singularity in its derivatives and can be expected to be identified by wavelet analysis. It can thus be concluded that the wavelet analysis can be helpful for both dynamic (mode) and static deflected shape.

4. Wavelet and Kurtosis Analysis

4.1 Wavelet Analysis

In a square integrable function space, a wavelet is a zero average function [6] satisfying

$$\int_{-\infty}^{+\infty} \psi(x)dx = 0 \tag{16.1}$$

A wavelet family of functions may be obtained by considering

$$\psi_{b,s}(x) = \frac{1}{\sqrt{s}}\psi(\frac{x-b}{s}) \tag{16.2}$$

where s is the scale and b is the translation parameter. The continuous wavelet transform of a function f(x) in the same square integrable space can be represented as

$$Wf(b,s) = \int_{-\infty}^{+\infty} f(x)\frac{1}{\sqrt{s}}\psi^*(\frac{x-b}{s})dx \tag{16.3}$$

where ψ^* is the complex conjugate of ψ.

The Calderon-Grossman-Morlet theorem [1] requires a weak admissibility condition to ensure the completeness of the wavelet transform and to maintain energy balance. Mathematically, it is represented as

$$\int_{0}^{+\infty} \frac{|\hat{\psi}(\omega)|^2}{\omega} d\omega < +\infty \tag{16.4}$$

The identification of a discontinuity in a function or any of its derivatives can be linked with the number of vanishing moments of the wavelet basis function chosen for analysis. A wavelet has m number of vanishing moments if

$$\int_{-\infty}^{+\infty} x^k\psi(x)dx = 0, \quad k=0,1,2\ldots m\text{-}1 \tag{17}$$

For a wavelet with no more than m number of vanishing moments, it can be shown that for very small values of s in the domain of interest, the continuous wavelet transform of a

function f(x) can be related to the m^{th} derivative of the signal [6]. For any wavelet $\psi(x)$ with m vanishing moments, there exists a fast decaying function $\zeta(x)$ satisfying:

$$\psi(x) = (-1)^m \frac{d^m \zeta(x)}{dx^m} \tag{18.1}$$

Under this condition, the relationship between the continuous wavelet transform of f(x) and its m^{th} derivative can be expressed as

$$\lim_{s\to 0} \frac{Wf(b,s)}{s^{m+1/2}} = K \frac{d^m f(x)}{dx^m} \tag{18.2}$$

where:

$$\int_{-\infty}^{+\infty} \zeta(x)dx = K \neq 0 \tag{18.3}$$

It is possible for a wavelet to detect singularities in a signal or its derivatives through the incorporation of a basis function having an appropriate number of vanishing moments according to the discontinuity present at the location of damage in the damaged beam model [2, 22]. For example, considering a lumped crack model, a basis function with one vanishing moment (like Haar) would introduce a jump at the damage location in the wavelet coefficients, whereas a basis function with more than one vanishing moment would generate an extremum. As per Mallat [1], a Gaussian function or its derivatives are guaranteed to detect the singularities even at very fine scales. In this paper however, Coiflet basis functions have been used and very good results have been obtained. The calibration of damage can be associated with the absolute value of the maxima of wavelet coefficients at different scales at the location of damage in the beam.

An alternative way of damage calibration is related to evaluating the kurtosis of the fundamental modeshape. Since the effect of the crack is local, the fundamental

modeshape and its central moments change very little. However, the kurtosis is affected even by the small change in modeshape comparatively more for the same amount of change in the modeshape itself and is thus considered suitable for calibrating the damage extent.

4.2 Kurtosis

Kurtosis represents the degree of peakedness of a dataset and is represented as a ratio of the fourth central moment of the data to its squared variance. This normalized form of the fourth central moment for the modeshape can be expressed as

$$\beta = \frac{\int_0^L (x-\bar{\mu})^4 \Phi(x)dx}{(\int_0^L (x-\bar{\mu})^2 \Phi(x)dx)^2} \tag{19}$$

where $\bar{\mu}$ represents the mean value of the modeshape. Considering the i^{th} moment of a function to be μ_i, it can be shown that

$$\frac{\partial \beta}{\partial x} = \frac{\mu_4' \mu^2_2 - 2\mu_2 \mu_4 \mu_2'}{\mu^4_2} \tag{20}$$

to compare the sensitivity of the kurtosis measure with the different moments of a function. A test function Y(x) = Sin(x) considered within limits 0 and 1. The first ten moments of this function and their partial derivatives with respect to x are given in Table 1 along with the values of kurtosis and its derivative. It is observed that the measure of kurtosis is more suitable to describe a small change in the function in comparison with the central moments. Since the first modeshape of a damaged beam is close to a sinusoid

with some small additive terms affecting the function locally near the damaged region, it is expected that the kurtosis based damage quantification is appropriate and effective.

With the introduction of damage, a slope discontinuity is introduced in the signal. For a significant change in slope, a change in kurtosis is observed as well [14].

4.3 Signal to Noise Ratio (SNR)

Wavelet based and kurtosis based calibrations are required to be consistent and stable in the presence of measurement noise to be efficient and robust. The effect of the presence of noise in the modeshape data has been studied by introducing synthetic Gaussian white noise to the simulated modeshape. Performance of the damage detection schemes are studied for different signal to noise ratio (SNR) values.

The SNR is defined as

$$SNR=10\log_{10}\left(\frac{P_{Signal}}{P_{Noise}}\right) \tag{21.1}$$

and is expressed in decibels. The term P with the subscripts in Equation 20.1 denotes power and is computed as

$$P_{(.)}=\frac{1}{N_S}\sum_{i=0}^{N_S-1}\left|f(x_i)\right|^2 \tag{21.2}$$

where N_S denotes the number of discrete points in a sampled signal f(x).

A high signal to noise ratio indicates that the presence of noise is very low and vice versa.

5. Wavelet Based Damage Detection

5.1 Wavelet Analysis of Modeshape

Damaged modeshape data is simulated and Gaussian white noise is synthetically introduced. The length of the beam is taken as 1 m. The cross sectional area (A), depth (h) and the moment of inertia (I) of the square beam are taken as 0.0001 m^2, 0.01 m and $8.33x10^{-10}$ m^4 respectively. The Young's modulus (E) and the density of the beam (ρ) are assumed to be $190x10^9$ N/m^2 and 7900 kg/m^3. The modeshape is analysed by Coif4 wavelet basis function, which has eight vanishing moments, and hence is suitable for damage detection. The modeshape data is multiplied by a Hanning window of length equal to that of the modeshape data to reduce edge effects and enhance the performance of wavelet based identification of damage location under the presence of noise.

Identification of small and edge cracks usually pose a major problem in damage detection. Figures 1.1 to 1.4 show the performance of wavelet based damage identification techniques for different crack depth ratios and locations with modeshapes simulated considering different crack models. Both fine (2, 3 and 4) and coarse (16, 32, and 64) scales have been considered for the purpose of identification. The SNR is kept at 125 dB to illustrate the efficiency of the wavelet based damage detection on a relatively pure signal. The high value of SNR ensures efficiencyIt is observed that the wavelet based identification of the damage location is efficient and consistent irrespective of the crack model chosen as long as it can identify a sudden local change in the signal. Figure 1.1 serves the purpose of illustrating the sensitivity of wavelet based damage location identification. Detection of such small edge cracks ensures successful identification of structurally more important cracks (Figure 1.3). Wavelet analysis on the modeshape derived from the smeared crack model identifies an open crack located in between the

position of the two local extrema of the wavelet coefficients and thus provides an upper bound of the estimate of the width of the damaged region (Figure 1.4).

It is observed from Figures 1.1 to 1.4 for different crack models, that an extremum of the wavelet coefficients is formed at the damage location, but the magnitude of it is extremely small in the case of small, edge cracks and it is thus very difficult to identify the damage. The lower scales are more sensitive to small changes in the damage level and identify the damage location very accurately. However, the lower scales are more prone to the effect of masking under the presence of noise and the detection is expected to become difficult when noise is present. The higher scales have a comparatively poor sensitivity and localisation property with regard to the identification of damage, but they are more robust against noise.

The effects of the presence of noise have been discussed in the following sections. For the rest of the analysis in this paper a lumped cracked model has been considered.

5.2 Partial Windowing

The modeshape is simulated from the lumped crack model, partially windowed by a Hanning window and then analysed as described in Section 5.1. An edge crack with δ=0.35 is considered at a distance 0.1m from the left edge. It is assumed that no prior information about the location of crack is present. The modeshape has been analysed according to the methodology described in Appendix 2. Hanning window has been used for partial windowing together with Coif4 wavelet basis function. Since a central crack is more important structurally for the structure under consideration, the partial windowing is performed first in the central region and is then gradually moved away. This ensures the

detection of important cracks in a lesser number of trials. The symmetric partitioning also ensures that the number of searches span half the length of the beam. However, a wavelet analysis has to be done separately for each partition. Analysis of the entire modeshape by wavelets would give rise to large extrema of wavelet coefficients at the ends of the partitioned sections and would thus lead to difficulties in identification of damage by undermining the actual damage. Hence, only the partially windowed sections should be analysed. Figures 2.1 and 2.2 illustrate the improvement in damage identification by partial windowing for the present damage condition for SNR equal to 120 dB for scales 4 and 16 respectively. Figure 2.1 represents the analysis of the partitioned section at scale 4 as opposed to its non-partitioned counterpart and the local maxima of the wavelet coefficients are seen to be about an order higher in the case of partitioned analysis. Once, the damage location is found in this way, the absolute value of the maxima can be improved by centering the damage location around an arbitrarily thinner section of the multiplying window and repeating the wavelet analysis. However, a calibration based on such method would be dependent upon the choice of the centered thinner sections. It is also seen that for such centering, the finer scales respond considerably better through a significant increase in the local maxima value of the wavelet coefficients at the damage location. Partial windowing also works in the presence of noise even when the analyses involving finer scales are masked and the coarser scales (8, 16 and 32) are able to identify the damage location.

6. Damage Calibration

6.1 Wavelet Based Calibration

Since the magnitude of the local extremum at the damage location of the wavelet coefficients can be related to the extent of damage, a wavelet based calibration against crack depth ratio is performed by finer and coarser scales. Figure 3.1 considers a central crack located at 0.4m from the left hand support with 120dB SNR and is calibrated using Coif4 wavelet basis. It is seen that the relationship between the magnitude of local maximum and the crack depth ratio is consistent and stable. An edge crack, situated at 0.1m from the left edge however, gives inconsistent results at finer scales as shown in Figure 3.2. The level of noise is increased and the SNR is kept at 95dB next. For a central crack at a distance of 0.4m from the left hand support (Figure 3.3), the calibration with Coif4 basis at finer scales becomes inconsistent as masking effect substantially sets in. The effects of an edge crack at a distance 0.1m from the left support for the same basis and SNR are illustrated in Figure 3.4. It is observed that a complete masking takes place and the wavelet based calibration is unsuitable. It has also been found by considering several wavelet basis functions that the choice of the basis function does not affect the inconsistency under noise significantly, although the calibration values are different. Hence, it may be concluded that the wavelet based calibration is appropriate in the presence low noise. It is not robust, consistent or stable in the presence of high SNR. However, in terms of determining the crack location the wavelet based method is found to be very efficient.

6.2 Kurtosis Based Calibration

A kurtosis based calibration is investigated next. It is assumed that the location of the crack has been successfully identified by a wavelet based technique and only the extent

of damage needs to be calibrated. The kurtosis of the entire modeshape is first calculated as opposed to partitioning the modeshape by preselected and empirically adjusted overlapping windows of a certain width and then calculating the kurtosis of each section. Different crack depths and locations are considered under no noise and the crack depth ratio is calibrated against the kurtosis value, as shown in Figure 4. The calibration curves are found to be monotonic. However, the nature of monotonocity changes with the damage location and it is possible to find a point of damage location where the kurtosis values become insensitive to the increasing crack depth ratio. This is essentially because of the fact that the fundamental modeshape itself has a maximum value between the supports. A cantilever, on the other hand has the maximum value at its end and it is not possible to get a damage location where the kurtosis may become insensitive to the change of crack depth. Thus, the suitability of a kurtosis based damage calibration depends on the support conditions of the structure.

The kurtosis of a quarter of the modeshape multiplied by an appropriately and empirically placed Hanning window of width equal to that of the partial modeshape is computed next for a beam with lumped crack model for calibrating the extent of damage. The damage is located correctly at 0.15m from the left hand support of the beam by wavelet analysis with Coif4 wavelet basis function using finer scales. The SNR is 115dB. A comparison on the relative change of the kurtosis of the damaged modeshape with respect to the undamaged condition for both full and partial modeshapes for different crack depth ratios are presented in Table 2. It is observed that the percentage change in the kurtosis value of the partial modeshape is less than that of the entire modeshape. The problem of non-detection of damage extent in certain cases can, in principle be solved by

computing the kurtosis on a part of the modeshape, but that would make the calibration extremely case specific.

The efficiency of the kurtosis based calibration in the presence of noise is checked for different SNR and the position of the crack for crack depth ratios 0.35 and 0.05 respectively. The results are given in Figures 5.1 and 5.2 respectively. It is seen that a kurtosis based calibration is extremely stable and consistent against noise to a large degree. For SNR as low as about 35dB, the calibration is found to be stable and consistent. The values of the kurtosis are however, small since the modeshape geometry does change significantly due to the local effects of an open crack.

Since the extrema values of the wavelet coefficients at different scales consistently increase with the increase in damage extent in the beam, the kurtosis is computed directly on the transformed partial modeshapes multiplied with a Hanning window at a certain scale after wavelet analysis. The windows are empirically placed so that the central region matches with vicinity of the damaged location. Figures 6.1 and 6.2 show the calibration for the damaged beam for different damage locations, crack depth ratios and SNR at scale 4 using Coif4 wavelet basis function. A calibration based on the values of kurtosis of the wavelet transformed modeshapes is more sensitive towards the extent of damage and the SNR. The calibration of damage is observed to be dependent on the position, the type and extent of the damage, the support conditions of the structure, the signal to noise ratio, the width and the position of the window multiplied with the damaged shape and the type and the scale of the wavelet basis function used to analyse the damaged shape.

7. Experimental Validation

It is observed in principle that a wavelet-kurtosis based damage calibration can be useful to detect, isolate and identify an open crack. The noise present in the deflected shape affects the performance of the detection process. Experimental studies on damage detection with wavelets from static and dynamic deflected shape have been performed by Rucka and Wilde [23] and Patsias and Staszewski [24] using a camera based optical measurement technique. In this paper, we employ a video camera based damage detection technique followed by an intelligent pattern recognition procedure to identify, calibrate and compare the extent of damage using wavelet-kurtosis based methods. A simply supported aluminium beam of 1m length is employed for this purpose. The open crack is created by sawing a notch into the lower section of the beam of cross section 10mm x 10mm. The location of the damage is situated at 0.3m from the left hand support of the beam. The beam is vibrated freely by an arbitrary initial excitation and is simultaneously subjected to a static weight at the centre. The free vibration of the beam is recorded by an Olympus μ 800 digital camera. An appropriate deflected shape was chosen by running the video recording using a commercial software Ulead Video Studio 6 and freezing a single frame, a method similar to that employed by Hartman and Gilchrist [25]. The frame was converted and saved as a bitmap image of size 240 x 320 pixels and subsequently converted to black and white binary images by thresholding and the edges of the images were found using the Sobel method [26] incorporating the MATLAB 7.0 signal processing toolbox. The lower edge of the beam was detected from the image by an intelligent pattern recognition scheme. Figure 7.1 illustrates the general arrangement of the test. Figure 7.2 shows a thresholded and edge identified binary image representing

the partial deflected shape of a beam with an open crack (δ=0.5) of 2mm width at a certain instant of time during free vibration. The image consists of the deflected shape of the beam and some spurious environmental effects like the presence of shadow and experimental devices. The deflected shape is estimated from an intelligent pattern recognition process by isolating it from the spurious images. A wavelet analysis using Coif4 basis function and Hanning window is performed on the estimate of the deflected partial modeshape and the result of the analysis is presented in Figure 7.3. The horizontal axis of the observed value is pre-calibrated against the beam length and the damage is seen to be detected in the vicinity of 0.3m from the left hand side of the beam. The kurtosis of the transformed wavelet coefficients at scale 4 of the partial deflected shape is computed to be 34.37, which is in agreement with the theoretically calibrated value of 38.77. Hence, the proposed damage detection scheme is validated for real data and the method is proved independent of a damage model as long as the local changes near the damaged region can be measured by any sensor.

8. Conclusions

A detailed study has been presented regarding the importance of efficient and robust calibration of evaluating the position and extent of damage in structures. The presence and the location of damage have been found out by wavelet analysis performed on the first assumed natural mode of a simply supported beam with an open crack. Simulations based on the first modeshape and the static deflected have been used since it is convenient to measure the fundamental modeshape and the static deflected shape of real

structures. For obtaining the modeshape and the static deflected shape damage models of different levels of complexity have been used.

It is observed that a wavelet analysis technique on the mode or the static deflected shape of a structure can successfully identify the presence and the location of the damage. Partial windowing of the deflected shapes and consequent wavelet analysis of the segments is found to improve the local maximum values of wavelet coefficients to a certain extent.

A wavelet based calibration of damage is found to be prone to masking effect in the presence of noise. The finer scale calibrations are seen to be affected at a lower level of SNR as compared to the coarser scales. Even for moderate presence of noise, the calibration based on wavelet analysis is found to be inconsistent and unstable and is thus not suitable for use. A kurtosis based damage calibration is found to be stable and consistent in the presence of much higher amount of noise. The sensitivity of the values of the kurtosis based damage calibration has been improved by considering the kurtosis of the wavelet coefficients of the analysed deflected shape. The breakdown point of a kurtosis based measurement of the extent of damage has also been identified by calibrating against the SNR values. A novel, simple and inexpensive video camera based experiment has been performed on a simply supported aluminium beam with an open crack to illustrate the efficiency of the proposed theoretical method on real data.

It is observed that although a wavelet based method is suitable for identifying the damage presence and location efficiently, a kurtosis based damage calibration is comparatively much more suitable and robust. Hence, a wavelet based damage detection process in conjunction with a kurtosis based damage calibration is deemed practical and

useful considering the presence of measurement noise in the static or dynamic deflected shape data of a structure.

References

1. Mallat S, 2001, *A Wavelet Tour on Signal Processing*, Academic Press, New York
2. Gentile A and Messina A, *On the Continuous Wavelet Transforms Applied to Discrete Vibrational Data for Detecting Open Cracks in Damaged Beams*, International Journal of Solids and Structures, 2003, 40, 295-315
3. Loutridis S, Douka E and Trochidis A, *Crack Identification in Double Cracked Beams using Wavelet Analysis*, Journal of Sound and Vibration, 2004, 277, 1025-1039
4. Chang C.C and Chen L.W, *Vibration Damage Detection of a Timoshenko Beam by Spatial Wavelet Based Approach,* Applied Acoustics, 2003, 64, 1217-1240
5. Okafor A.C and Dutta A, *Structural Damage Detection in Beams by Wavelet Transforms*, Smart Materials and Structures, 2000, 9, 906-917
6. Melhem H and Kim H, *Damage Detection in Concrete by Fourier and Wavelet analyses*, ASCE Journal of Engineering Mechanics, 2003, May, 571-577
7. Kim H and Melhem H, *Damage Detection of Structures by Wavelet Analysis*, Engineering Structures, 2004,26, 347-362
8. Wang Q and Deng X, *Damage Detection with Spatial Wavelets,* International Journal of Solids and Structures, 1999, 36, 3443-3468
9. Hou Z, Nouri M and Amand R, *Wavelet Based Approach for Structural Damage Detection*, ASCE Journal of Engineering Mechanics, 2000, July, 677-683

10. Basu B, *Identification of Stiffness Degradation in Structures Using Wavelet Analysis,* Construction and Building Materials, 2005, 19, 713-721
11. Liew K.M and Wang Q, *Application of Wavelet Theory for Crack Identification in Structures*, ASCE Journal of Engineering Mechanics, 1998, February, 152-157
12. Moyo P and Brownjohn J.M.W, *Detection of Anomalous Structural Behaviour using Wavelet Analysis,* Mechanical Systems and Signal Processing, 2002, 16(2-3), 429-445
13. Hadjileontiadis L.J, Douka E and Trochidis A, *Fractal Dimension Analysis for Crack Identification in Beam Structures,* Mechanical Systems and Signal Processing, 2005, 19, 659-674
14. Hadjileontiadis L.J, Douka E and Trochidis A, *Crack detection in beam using kurtosis,* Computers and Structures, 2005, 83, 909-919
15. Narkis. Y, *Identification of Crack Location in Vibrating Simply Supported Beams*, Journal of Sound and Vibration, 1994, 172(4), 549-558
16. Masoud S, Jarrah M.A and Maamory M.L, *Effect of Crack Depth on the Natural Frequency of a Prestressed Fixed-Fixed Beam*, Journal of Sound and Vibration, 1998, 214(2), 201-212
17. Dado M.H, *A Comprehensive Crack Identification Algorithm for Beams under Different End Conditions*, Applied Acoustics, 1997, Vol. 51, No. 4, 381-398
18. Carneiro S.H.S, *Model-Based Vibration Diagnostic of Cracked Beams in the Time Domain*, PhD Thesis, Virginia Polytechnic Institute and State University, 2000

19. Carneiro S.H.S and Inman D.J, *Continuous Model for the Transverse Vibration of Cracked Timoshenko Beams*, Transactions of the ASME, Journal of Vibration and Acoustics, 2002, Vol. 24, 310-320
20. Shen M.H.H and Pierre C, *Free Vibration of Beams with a Single Edge Crack*, Journal of Sound and Vibration, 1994, 170(2), 237-259
21. Christides S and Barr A.D.S, *One-dimensional Theory of Cracked Bernoulli-Euler Beams*, International Journal of Mechanical Sciences, 1984, 26, 639-648
22. Bovsunovsky A.P and Matveev V.V, *Analytical Approach to the Determination of Dynamic Characteristics of a Beam with a Closing Crack*, Journal of Sound and Vibration, 2000, 235(3), 415-434
23. Rucka M and Wilde K, *Crack Identification using Wavelets on Experimental Static Deflection Profiles*, Engineering Structures, 2006, 28, 279-288
24. Patsias S and Staszewski W.J , *Damage Detection using Optical Measurements and Wavelets*, Structural Health Monitoring, Vol 1(1), 2002, 5-22
25. Hartman A.M and Gilchrist M.D, *Evaluating Four-Point Bend Fatigue of Asphalt Mix Using Image Analysis*, ASCE Journal of Materials in Civil Engineering, January-February, 2004, 60-68
26. Sarfraz M, *Computer Aided Intelligent Recognition Techniques and Applications*, 2005, John Wiley and Sons, Chichester, England

List of Tables

μ_i	$\frac{\partial \mu_i}{\partial x}$	β	$\frac{\partial \beta}{\partial x}$
0.0898	0.4546	3.9997	-7.2507
0.0435	0.2456		
0.0155	0.1327		
0.0076	0.0717		
0.0032	0.0387		
0.0016	0.0209		
0.0007	0.0113		
0.0004	0.0061		
0.0002	0.0033		
0.0001	0.0018		

Table 1.

	Full Modeshape	Change in %	Partial Modeshape	Change in %
δ=0.0	1.9311		1.4874	
δ=0.05	1.9324	0.07	1.4877	0.02
δ=0.20	1.9359	0.25	1.4883	0.06
δ=0.35	1.9416	0.54	1.4893	0.13

Table 2.

List of Figures

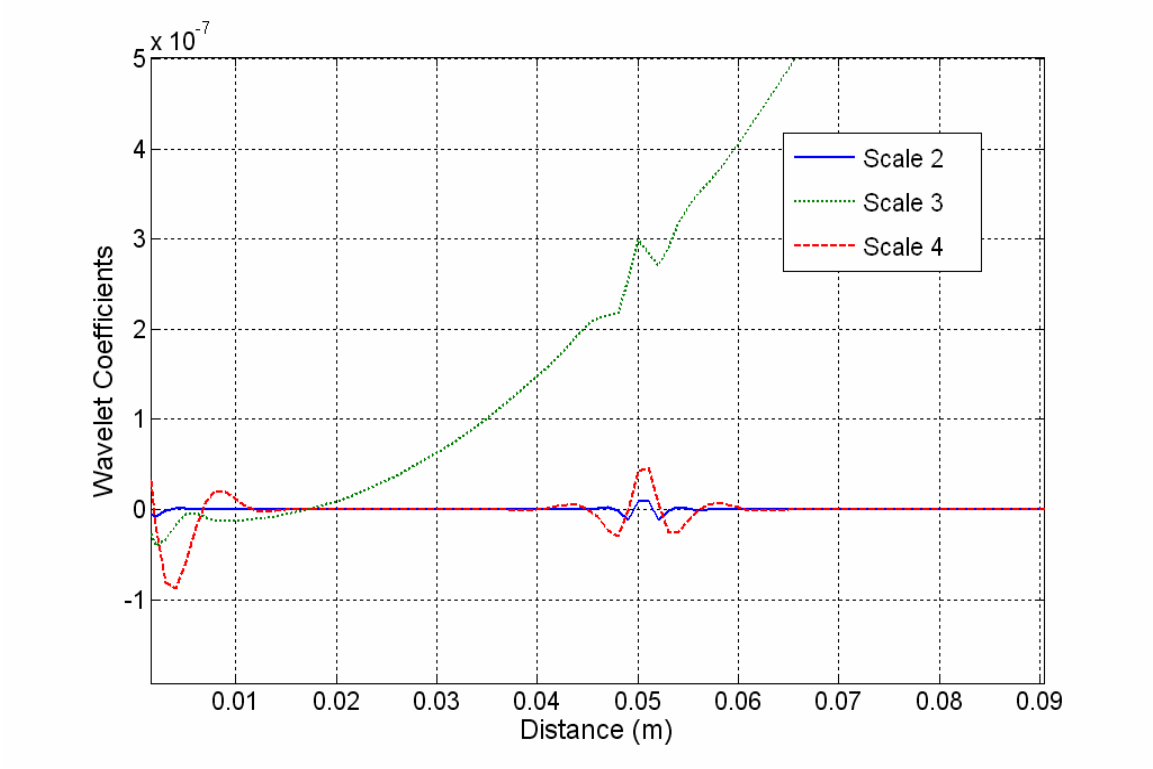
x 10^-7
5
4
3
2
1
0
-1
Wavelet Coefficients
0.01
0.02
0.03
0.04
0.05
0.06
0.07
0.08
0.09
Distance (m)
Scale 2
Scale 3
Scale 4

Figure 1.1

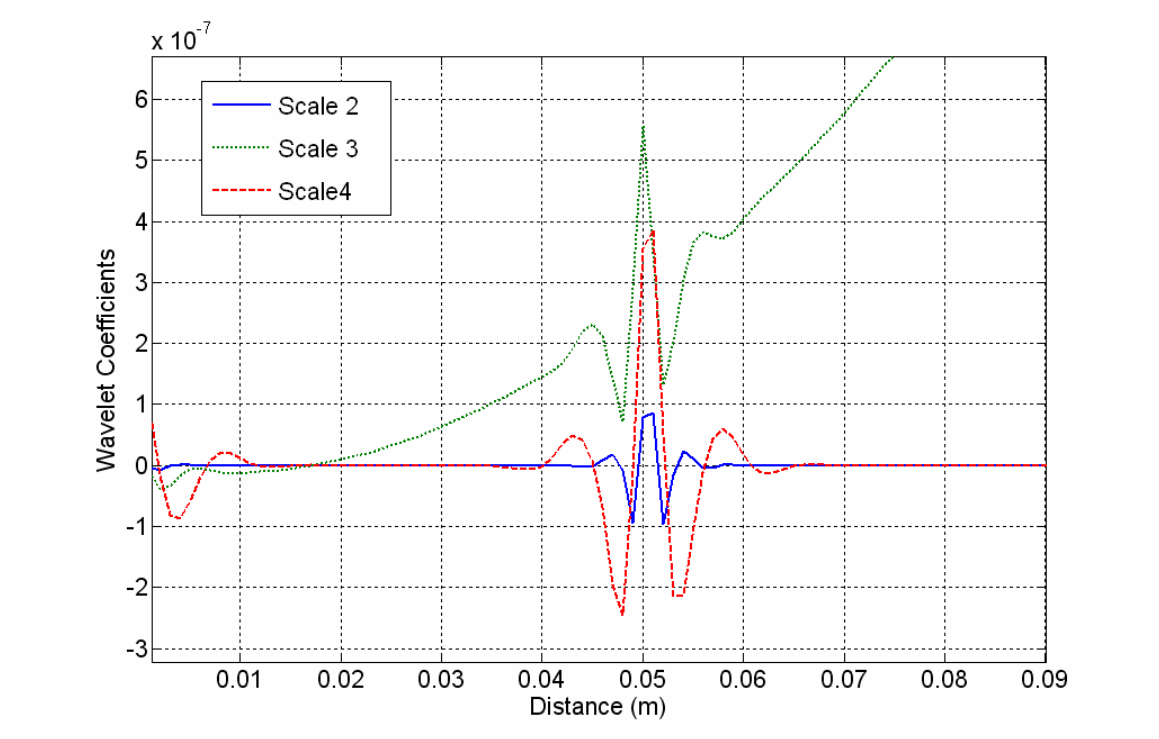
x 10^-7
Scale 2
Scale 3
Scale4
Wavelet Coefficients
Distance (m)
6
5
4
3
2
1
0
-1
-2
-3
0.01
0.02
0.03
0.04
0.05
0.06
0.07
0.08
0.09

Figure 1.2

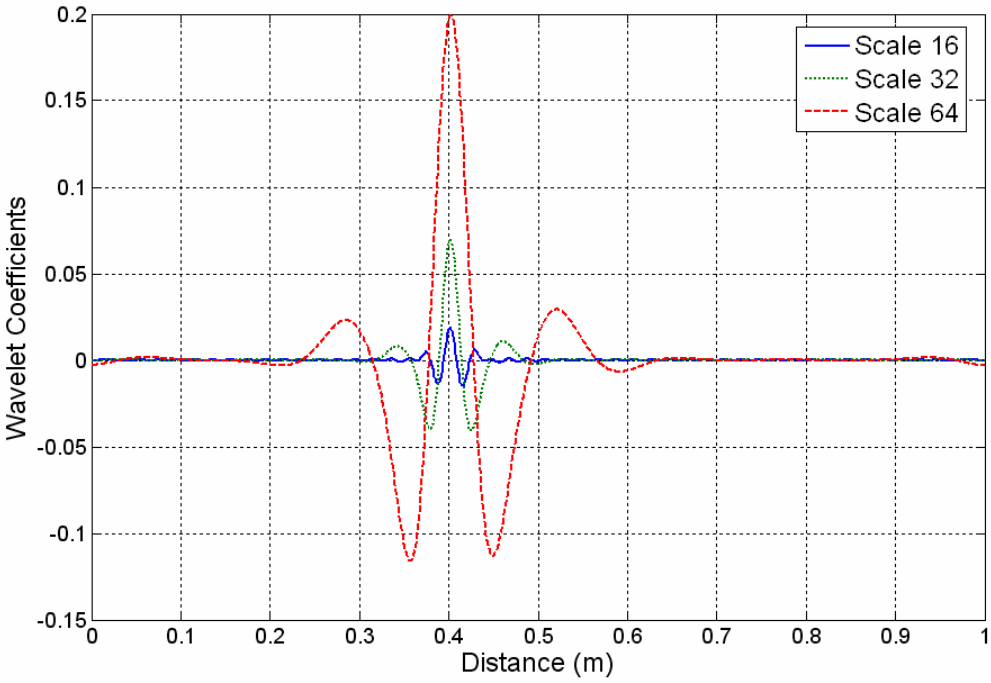
Scale 16
Scale 32
Scale 64
Wavelet Coefficients
Distance (m)
0.2
0.15
0.1
0.05
0
-0.05
-0.1
-0.15
0
0.1
0.2
0.3
0.4
0.5
0.6
0.7
0.8
0.9
1

Figure 1.3

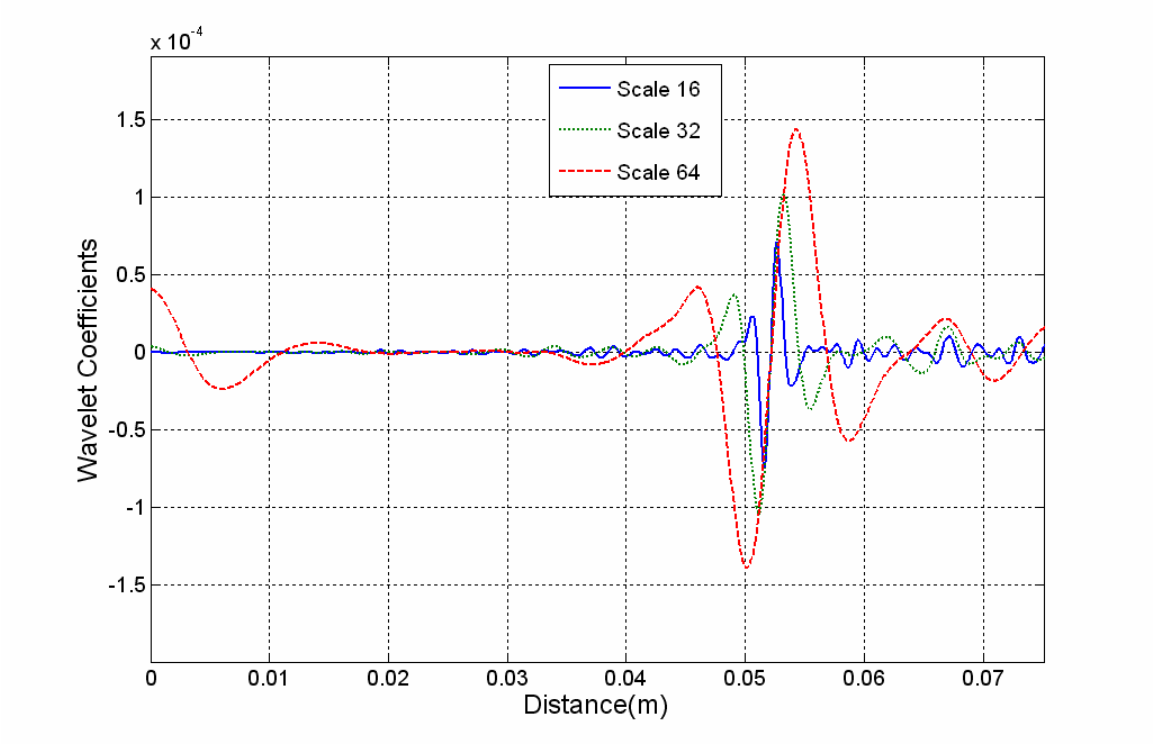
x 10^-4
Scale 16
Scale 32
Scale 64
Wavelet Coefficients
1.5
1
0.5
0
-0.5
-1
-1.5
0
0.01
0.02
0.03
0.04
0.05
0.06
0.07
Distance(m)

Figure 1.4

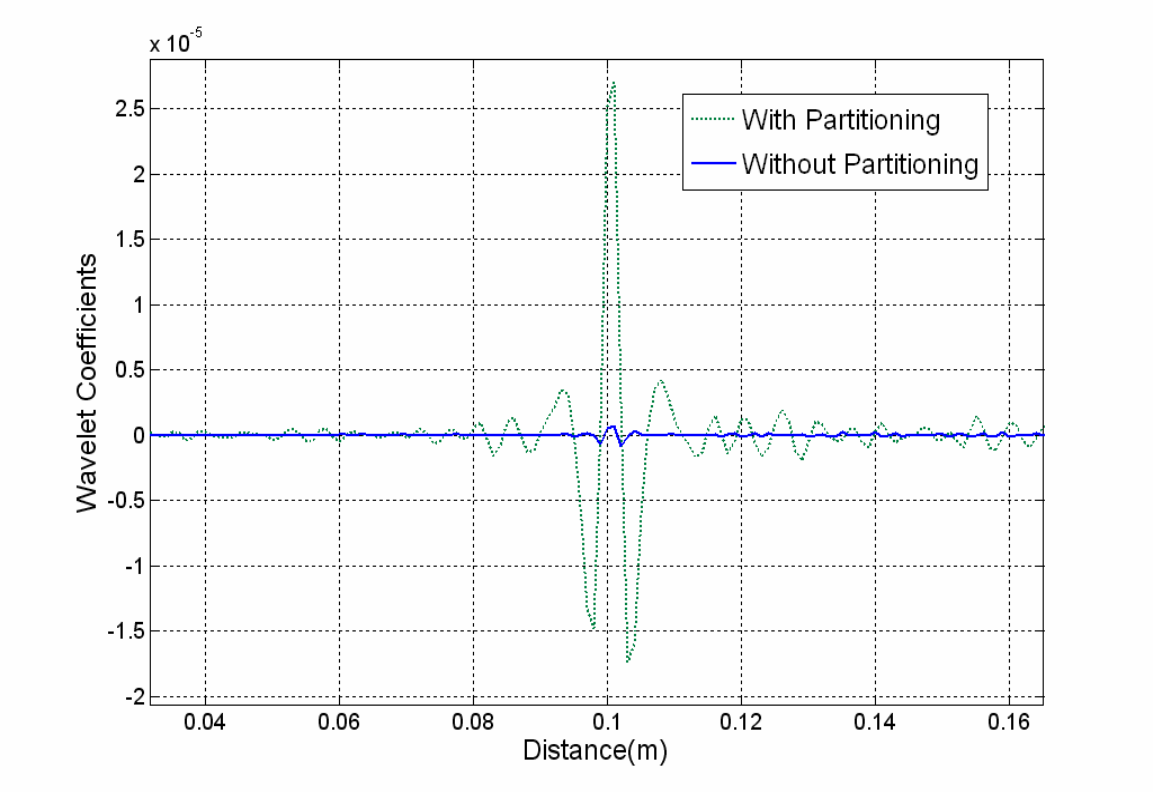
x 10^-5
2.5
2
1.5
1
0.5
0
-0.5
-1
-1.5
-2
Wavelet Coefficients
0.04
0.06
0.08
0.1
0.12
0.14
0.16
Distance(m)
With Partitioning
Without Partitioning

Figure 2.1

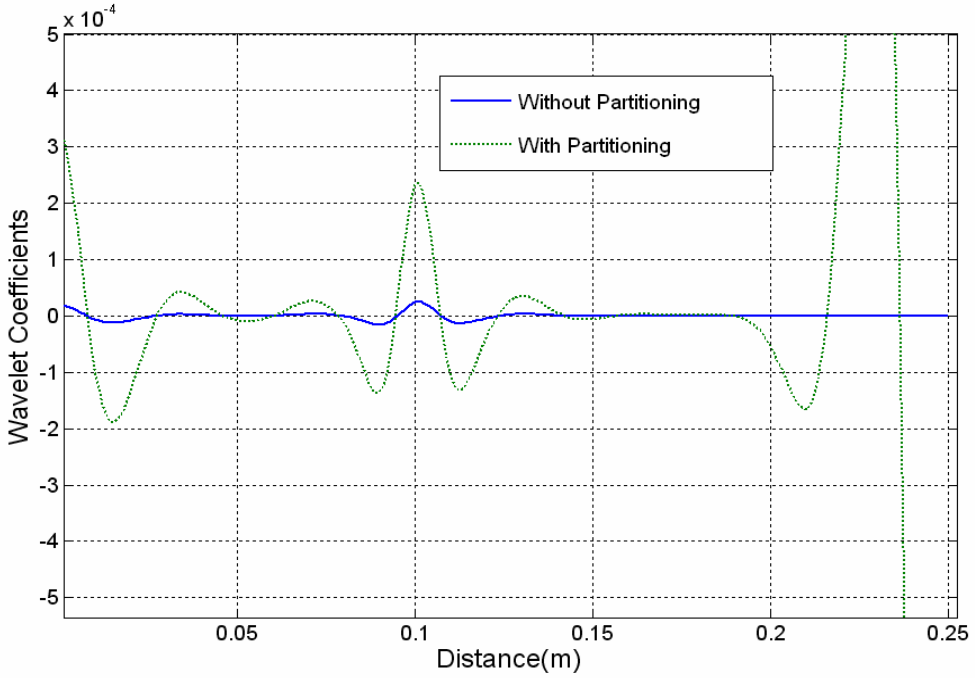
x 10^-4
5
4
3
2
1
0
-1
-2
-3
-4
-5
Wavelet Coefficients
0.05
0.1
0.15
0.2
0.25
Distance(m)
Without Partitioning
With Partitioning

Figure 2.2

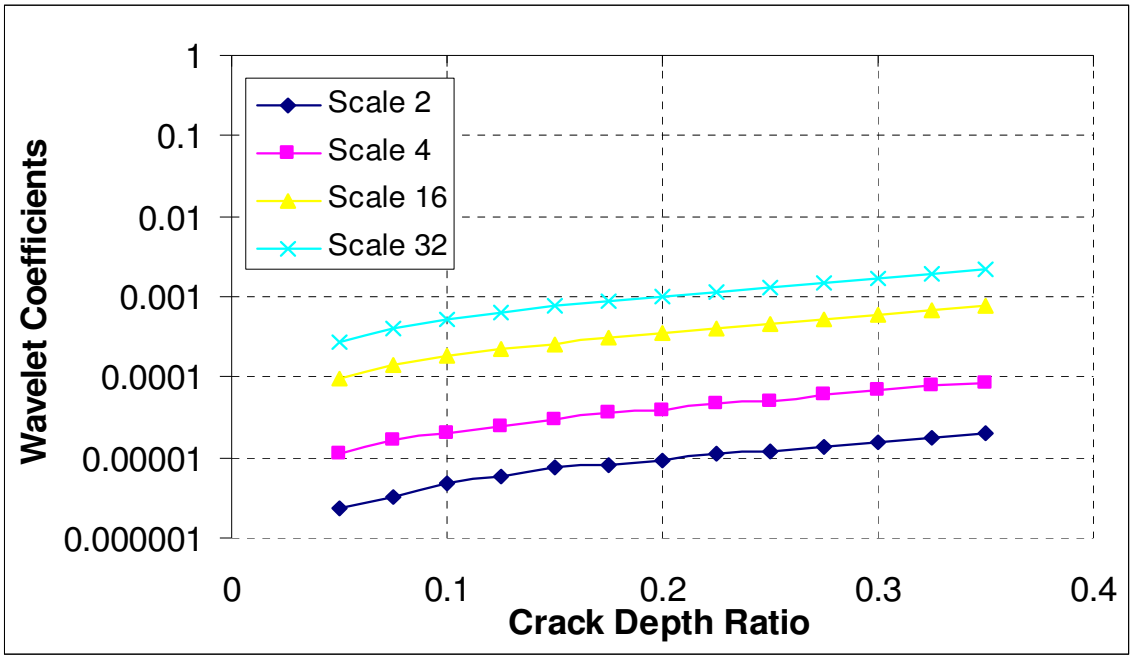

Figure 3.1

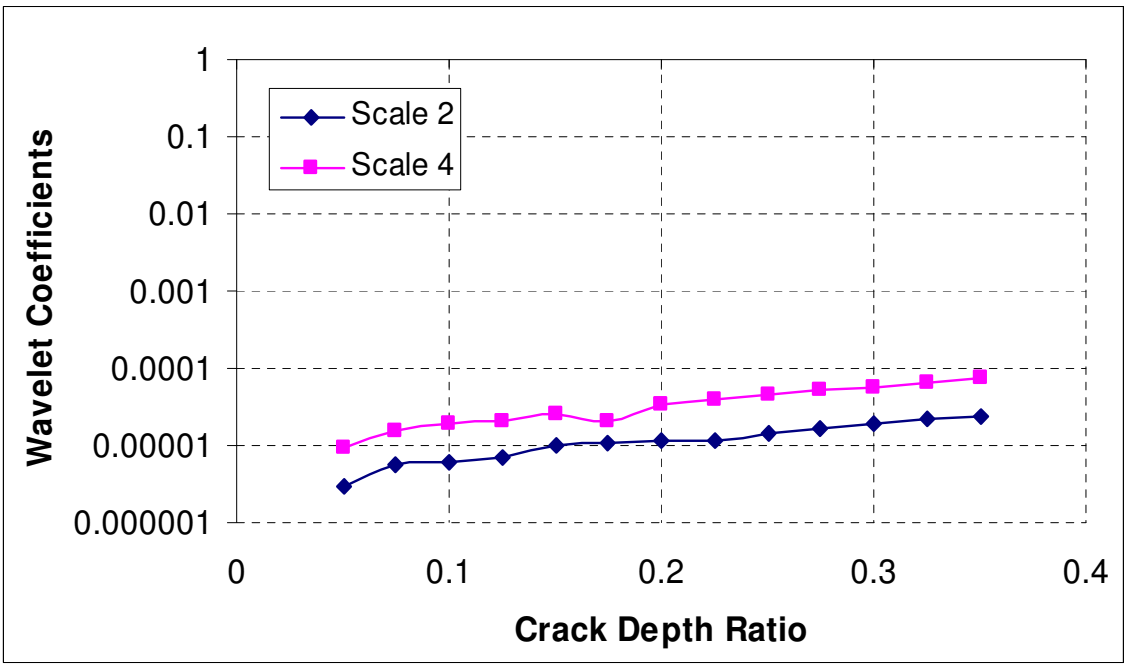

Figure 3.2

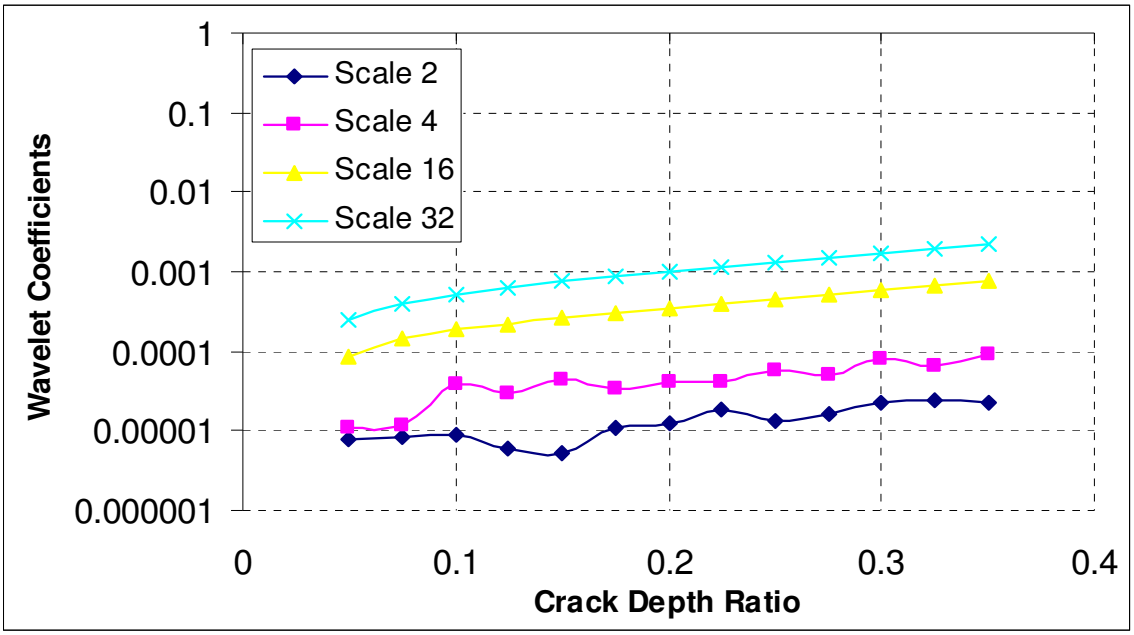

Figure 3.3

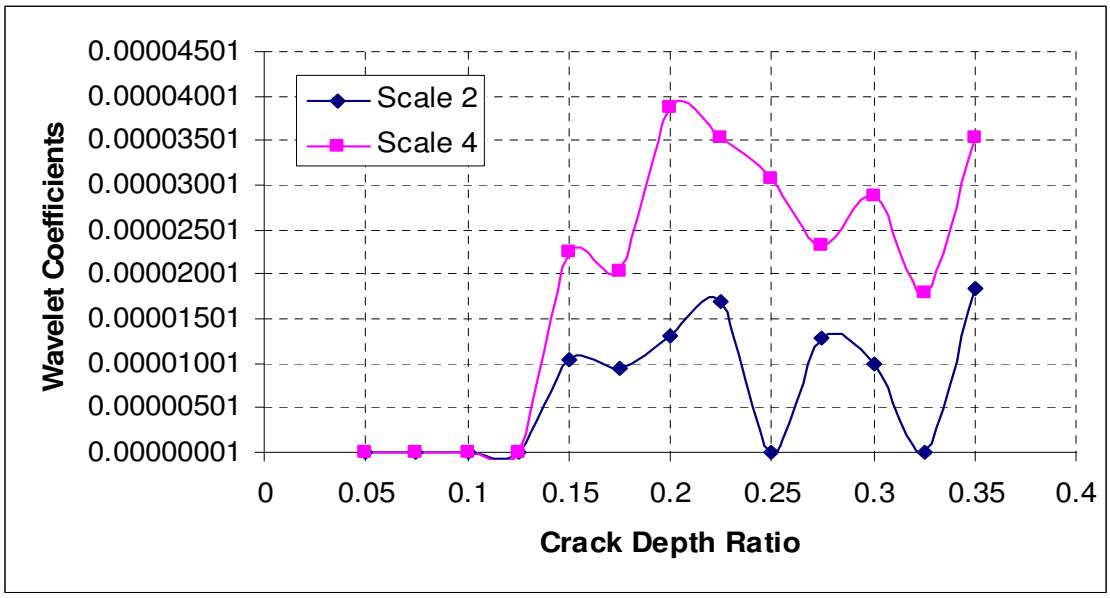

Figure 3.4

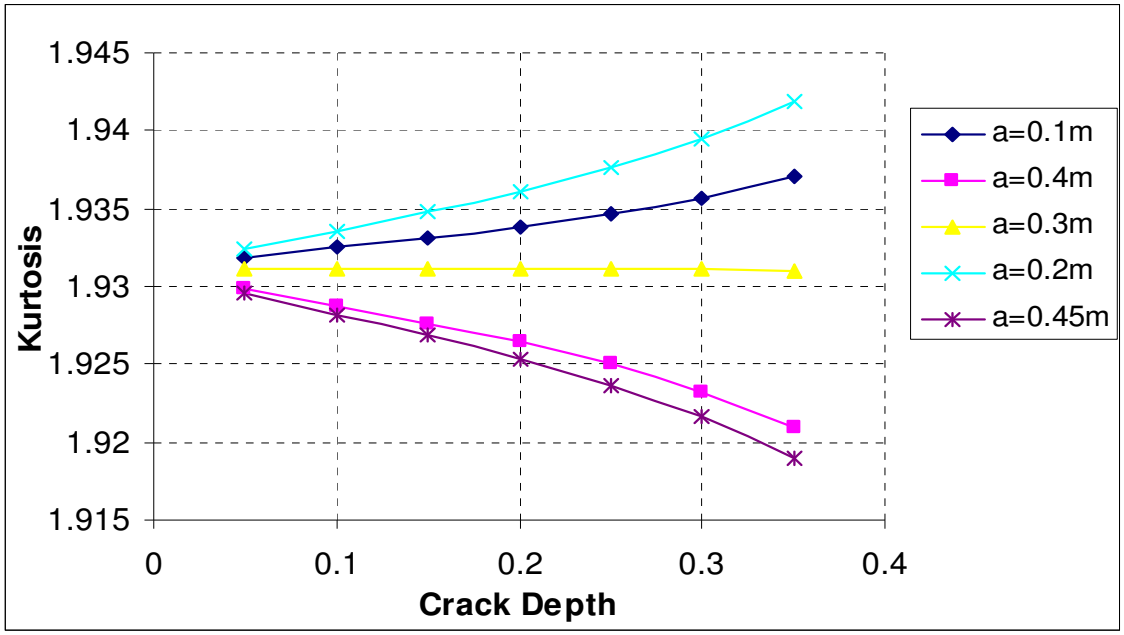

Figure 4

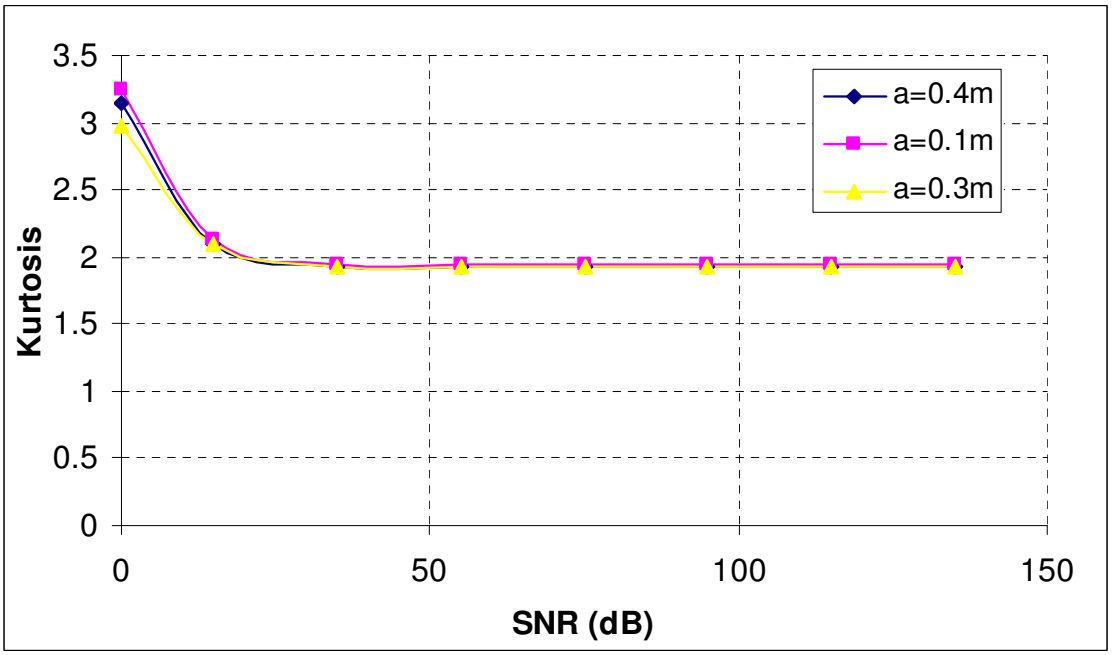

Figure 5.1

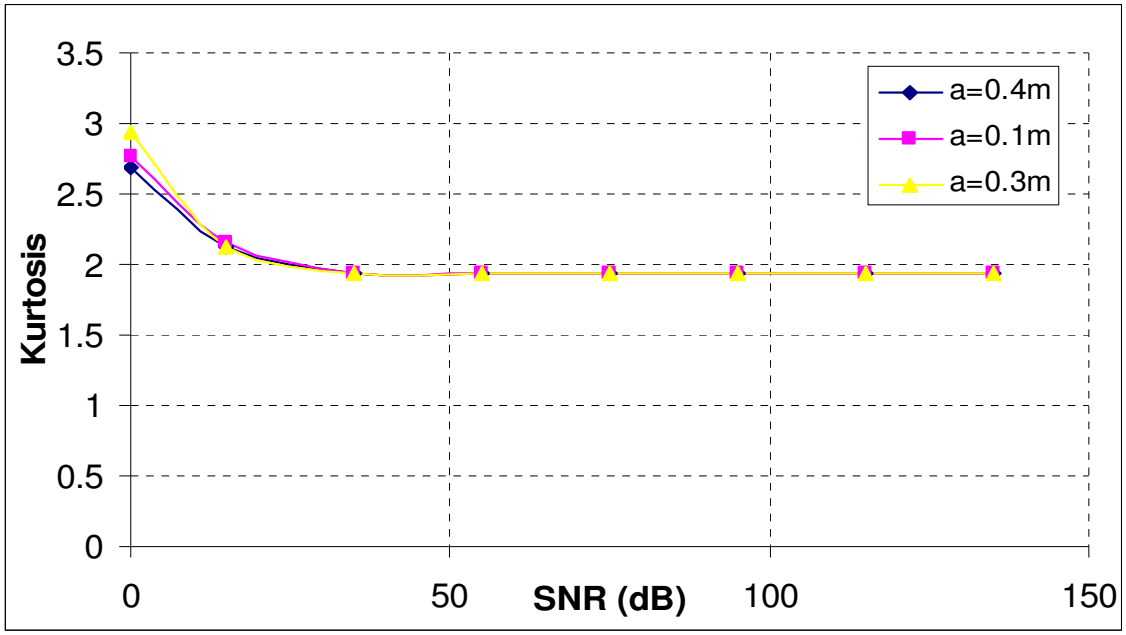

Figure 5.2

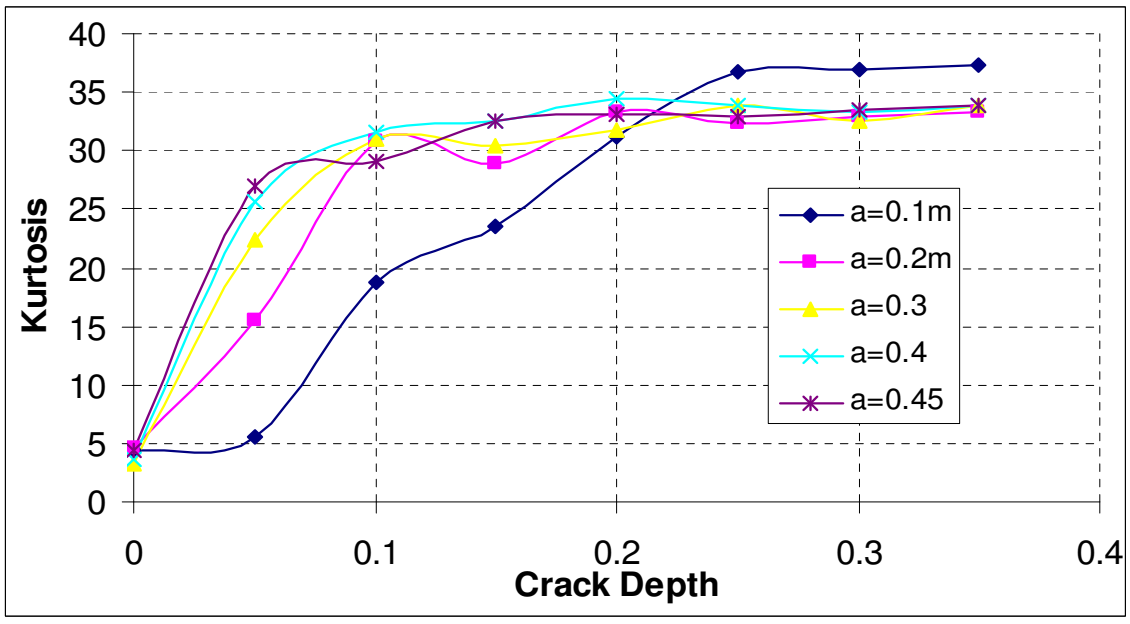

Figure 6.1

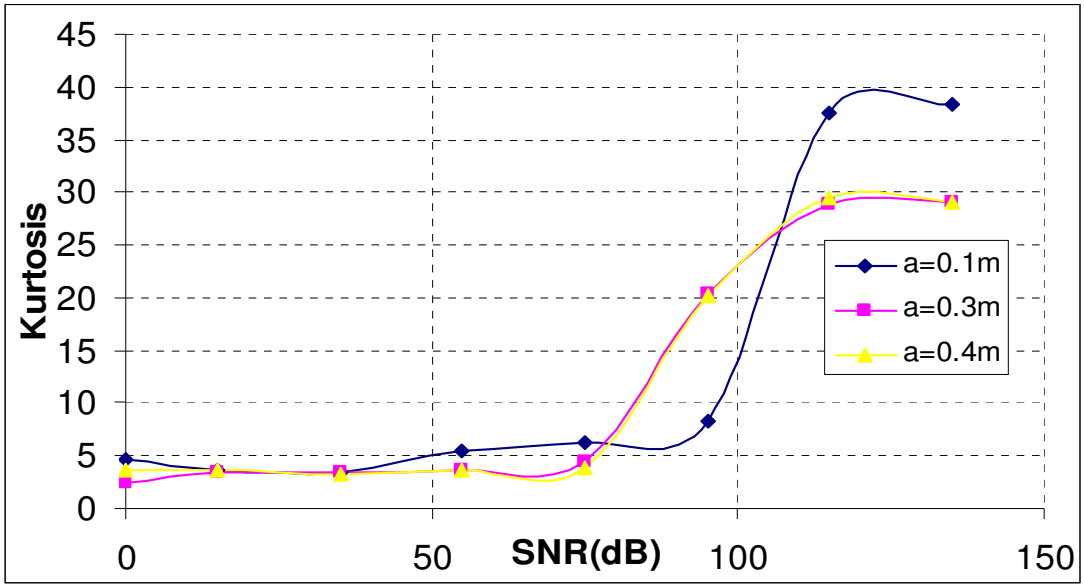

Figure 6.2

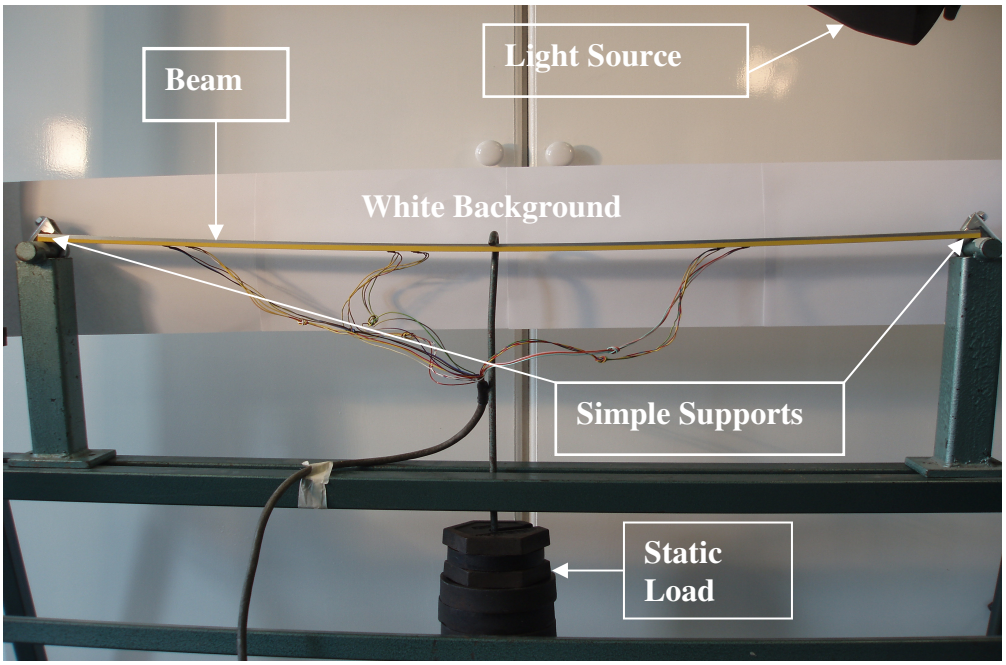

Figure 7.1

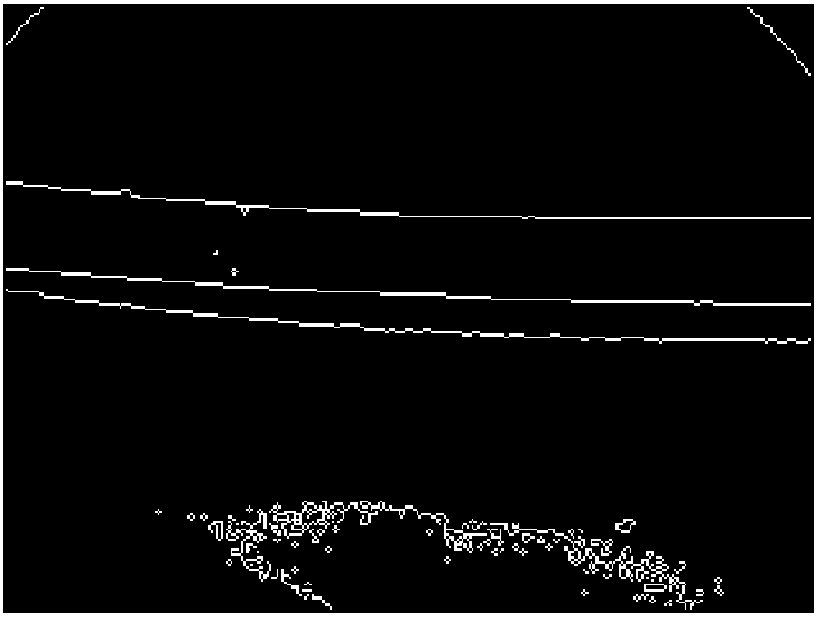

Figure 7.2

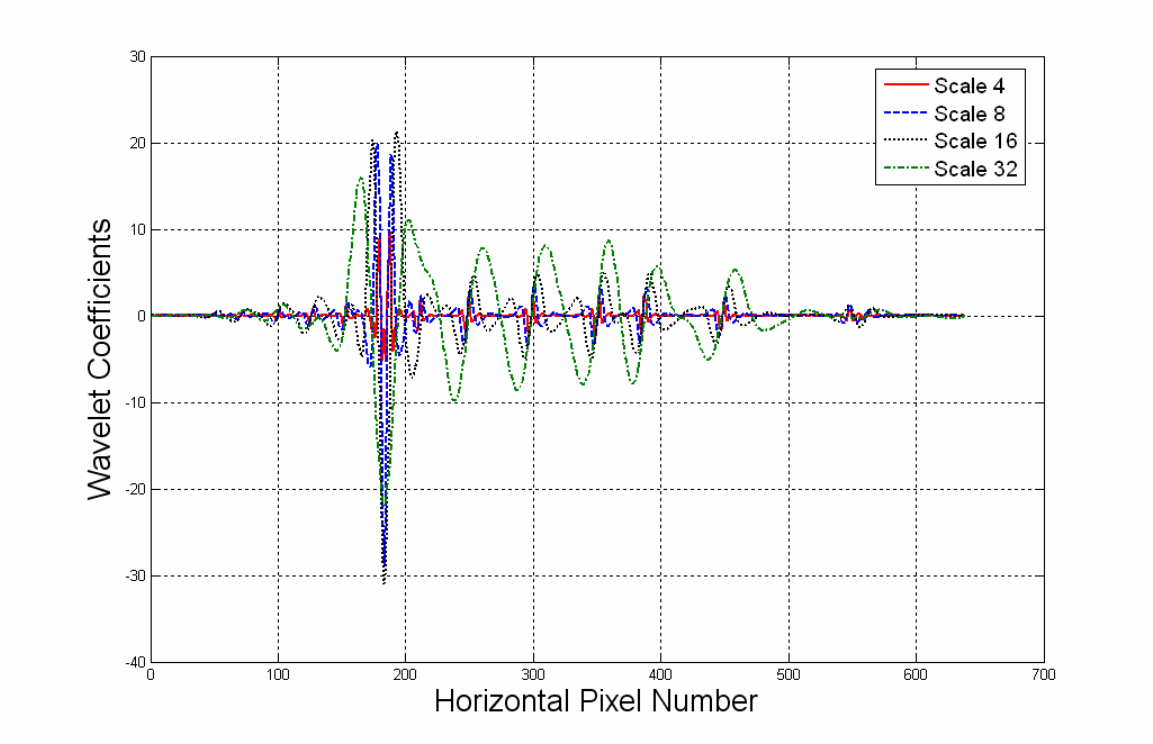
Scale 4
Scale 8
Scale 16
Scale 32
Wavelet Coefficients
Horizontal Pixel Number
30
20
10
0
-10
-20
-30
-40
0
100
200
300
400
500
600
700

Figure 7.3

Appendix 1

Coefficients $p_1(x)$ *and* $p_2(x)$ *for the continuous cracked model.*

$$p_1(x) = E[\{I - \int_A z f_1(x,z)dA - \int_A z f_2(x,z)dA + \int_A f_1(x,z) f_2(x,z)dA\}(\frac{\int_A f_1(x,z) f_2'(x,z)dA) - (\int_A z f_2(x,z)dA)'}{I - 2\int_A z f_1(x,z)dA + \int_A f_1^{\,2}(x,z)dA})' +$$

$$\{(\int_A f_2(x,z) f_1'(x,z)dA))' - (\int_A z f_1(x,z)dA)''\}(\frac{\int_A f_1(x,z) f_2'(x,z)dA) - (\int_A z f_2(x,z)dA)'}{I - 2\int_A z f_1(x,z)dA + \int_A f_1^{\,2}(x,z)dA})]$$

$$p_2(x) = [I - \int_A z f_1(x,z)dA - \int_A z f_2(x,z)dA + \int_A f_1(x,z) f_2(x,z)dA](\frac{I - \int_A z f_1(x,z)dA - \int_A z f_2(x,z)dA + \int_A f_1(x,z) f_2(x,z)dA}{I - 2\int_A z f_1(x,z)dA + \int_A f_1^{\,2}(x,z)dA})$$

Appendix 2

Scheme of Partial Windowing Method for Efficient Wavelet Based Damage Detection

1. Acquire the damaged modeshape/deflected shape from simulation or experiment.
2. Divide the modeshape into a finite number of partition equal to 2^i starting with the value i=1.
3. Multiply an appropriate window of length equal to length of the finite partition to each of the finite partitions.
4. Construct a system of 2^{i+1}-1 overlapping windowed partition covering the entire length of the beam. The central partition is symmetric about the centre of the beam and the other 2^{i+1}-2 partitions are symmetrically placed about the centre with the end point of each partition coinciding with the maxima value of the other except at the two ends where they coincide with the supports of the beam.
5. Analyze each partially windowed shape using an appropriate wavelet basis.
6. Repeat the process of increasing the number of partitions till crack/cracks is/are identified or a preselected value of partitioning is reached indicating no damage is present.
7. Once a crack is identified at a particular section, the width of the window is centrally adjusted about the location of the identified damage and a wavelet analysis is performed on that section to obtain an improved value of a local extremum/extrema at the damaged location(s) of the wavelet coefficients.